A Novel Algorithm for Solar Potential Estimation in Complex Urban Scenes

Partha P. Acharjee and Venkat Devarajan
The University of Texas at Arlington, Texas, USA

***Abstract*: Significant power demand is located in urban areas, where, theoretically, a large amount of building surface area is also available for solar panel installation. Therefore, property owners and power generation companies can benefit from a citywide solar potential map, which can provide available estimated annual solar energy at a given location. An efficient solar potential measurement is a prerequisite for an effective solar energy system in an urban area. In addition, the solar potential calculation from rooftops and building facades could open up a wide variety of options for solar panel installations. However, complex urban scenes make it hard to estimate the solar potential, partly because of shadows cast by the buildings. LiDAR-based 3D city models could possibly be the right technology for solar potential mapping. Although, most of the current LiDAR-based local solar potential assessment algorithms mainly address rooftop potential calculation, whereas building facades can contribute a significant amount of viable surface area for solar panel installation. In this paper, we introduce a new algorithm to calculate solar potential of both rooftop and building facades. Solar potential received by the rooftops and facades over the year are also investigated in the test area.**

***Index Terms*— LiDAR, Solar power, Shadow mapping**

I. INTRODUCTION

The high population density and the vast availability of current technologies are common in urban areas, which make urban areas high-demand areas for electricity. Generating electricity locally through solar panels rather than transmitting from long distance is beneficial for the power system. Recent advances in solar power technologies, as well as green-power friendly governments policies, are also encouraging individual households to pursue their own solar power generation systems.

An estimation of available annual solar potential is important to make a confident power planning decisions. Especially, small households will come forward if a better picture of cost and benefit can be drawn. Although, the amount of sunlight striking a specific location is dependent on many factors e.g. surrounding structures, sun position, season and other meteorological factors. Additionally, in the urban landscape, estimating the solar potential becomes more challenging because of the abrupt change of surrounding structures.

The accurate elevation map of the landscape is a prerequisite for generating a city model, which can be used for shadow estimation and solar potential visualization over the terrain. Light detection and ranging (LiDAR) technology have few inherent benefits for this application. Highly accurate elevation maps from LiDAR returns can be used to generate a 3D model of the urban scenes. However, the solar power estimation becomes challenging if building facades are considered. In an urban scene, building facades provide an enormous amount of surface area for solar panel installation. Additionally, emerging solar panel technologies and government policies encourage installing solar panels on all available surfaces including the glass wall and the building facades. However, elevation of the side of buildings is not readily available from LiDAR point cloud. Additionally, estimating shadow on vertical planes make this task challenging.

The Solar Analyst from ArcGIS and r.sun from GRASS are two well-known solar power estimation tools using raster based elevation data [1, 2]. These tools are capable of estimating solar power on large areas from digital terrain models. Vertical surfaces are ignored in estimating solar potential in both of these tools. Some work has been performed to estimate solar power obtainable from vertical planes using the 2.5D elevation information from LiDAR data using assumptions that the facades are planar, and, discontinuities due to windows, balconies, and other irregular features are ignored [3, 4]. Despite these assumptions, the annual solar power per unit facade is an important factor.

In this paper, we present a new algorithm for solar power estimation in an urban scene, which considers both rooftops and building facades as potential places for solar panels. We also investigate how much additional power the building facades offer, and which facades have better solar potential at different times of the year.

II. PROPOSED ALGORITHM

In this proposed algorithm, a rasterized digital surface model was produced from LiDAR elevation data. Although 2m-by-2m raster size was used in this paper, which can be changed based on LiDAR data density and desired output resolution. The basic workflow of the algorithm is shown in Fig.1. First, all rooftops were detected using our previous work in [5]. The rasterized LiDAR data was given as input to the 3D city modeling block to detect all rooftops and facades. Sequentially, four adjacent points from the raster was taken by the build patches block to make a patch—a quadrilateral surface. Solar power was estimated for each these patches. Sun position, the azimuth and the elevation angle was calculated using an astronomical model. A typical meteorological year (TMY) dataset was used to get the solar intensity variation over time. All of this information was used to estimate the direct and the diffuse sunlight intensity on patches, where the orientations of patches were known from the LiDAR data.

The global radiation on rooftops and facades were derived from the direct and diffuse radiation model. In this paper, an

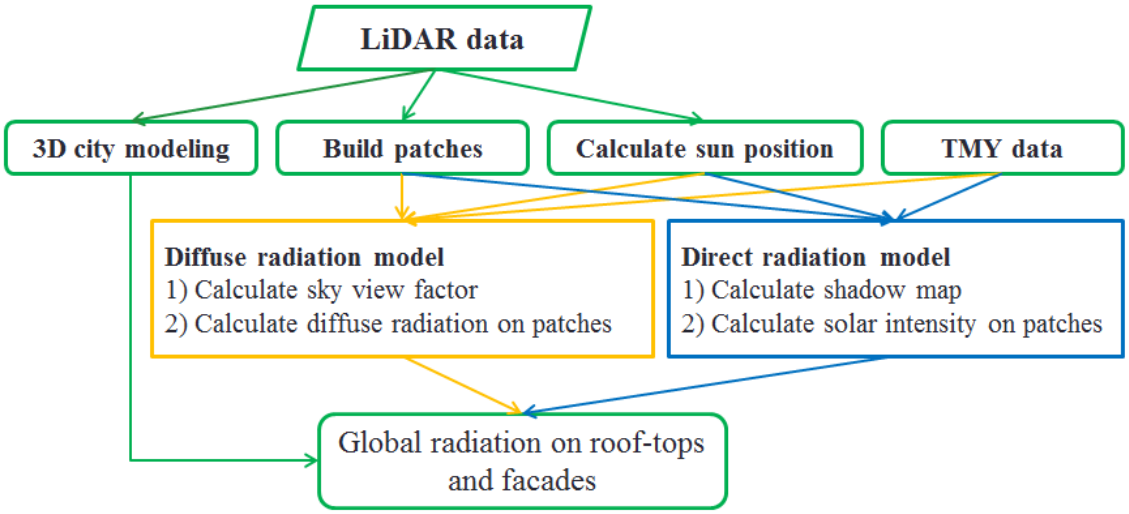

Fig. 1. Overall flowchart of the global solar radiation calculation on rooftops and facades from LiDAR data.

area from Dallas-Fort worth (DFW) region was used to demonstrate results. A test data from the same area, which has two buildings side by side, was used to demonstrate the basic concepts of the algorithm. Details of each block will be given in the following sections.

A. 3D city modeling

Detection of building rooftops and facades were important to estimate solar energy on those planes. In this algorithm, we used an angular filter based building detection method as given in [5]. Here, a short overview of the building detection method is given here. The building detection method detects all building edges based on the angular filtering method. Edges from each building were grouped together by using a connected component analysis. Each building area was enclosed by a convex hull, and the areas outside of the convex hulls were used to interpolate the elevation beneath the building. Based on the elevation difference, all rooftops planes were detected. Therefore, the 3D city modeling block provides the location of all buildings.

B. Build patches

Rasterized LiDAR data is a 2.5D based representation, where all points were evenly placed in xy-plane and any point does not share the same x and y values. Here, x, y, and z mean latitude, longitude, and altitude respectively. However, to represent vertical walls, multiple points have to share the same x and y values with different z values. The 2.5D representation is suitable if only rooftops were considered for solar power estimation. Therefore, a new representation should be introduced to bring building facades in the scene. For this purpose, patches were used to represent each plane in the scene. Four adjacent points, e.g. (n, m) (n+1, m) (n+1, m+1) (n, m+1), are grouped together to make a patch. The order of the points was set in the counter-clockwise direction; therefore, the normal of each patch was in the upward direction. Azimuth and elevation angles of the normal vector and the area of the patch were also calculated for next steps. If elevation angle of the normal vector is less than a minimum threshold then it was deemed a facade. Facades were equally divided into sixty-four small patches. Therefore, solar intensity can be calculated separately for each of those small segments. In Fig.03, patches are shown in a different color based on the altitude of the patch. We can see that facades are made up by multiple patches in multiple elevation levels.

C. Calculate sun position

In this algorithm, parallelism of sunrays was assumed, which means sun rays were consider parallel for all point of the study area. Therefore, only one set of azimuth and elevation angle was enough to represent the sun position for the whole area. Latitude, longitude, time, and date were used as inputs in an astronomical model to calculate the azimuth

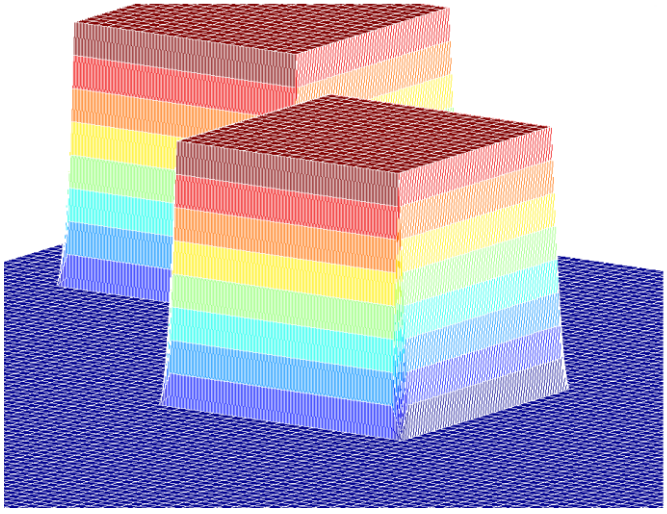

Fig. 2. Patches are color-coded by their elevation in the test dataset. Ground, rooftops and different height of the facades are shown in different colors.

and the elevation of the sun. Latitude and longitude of the area were available from the LiDAR data. The azimuth and the elevation angles were calculated as follows [6],

$$Elevation = \sin^{-1}\{sin\delta\ sin\varphi + cos\delta\ cos\varphi\ \cos(H)\}$$

$$Azimuth = \cos^{-1}\left\{\frac{sin\delta\ cos\varphi - cos\delta\ sin\varphi\cos(H)}{\cos(Elevation)}\right\}$$

Here, φ is the latitude δ is the declination angle and H is the hour angle, which was calculated from the time and longitude of the location in few steps. First, local standard time meridian (LSTM) was calculated from the time difference between the local and the GMT time as $LSTM = 15^{\circ} \times \Delta T$. The equation of time (EoT) was calculated from the day number (d) using the following equation,

$$EoT = 9.87\sin(2B) - 7.53\cos(B) - 1.5\sin(B)$$
$$where, B = \frac{360}{365}(d - 81)$$

The declination angle δ was calculated as $\delta = 23.45°sinB$. Then time correction factor (TC), local solar time (LST), and hour angle H were calculated as follows,

$$TC = 4(Longitude - LSTM) + EoT$$
$$LST = local\ time + \frac{TC}{60}$$
$$H = 15^{\circ}(LST - 12)$$

Positions of the sun at different time of the year were calculated using the above astronomical model. In Fig.02, sun positions are shown at the sky for the first day of each month in DFW area. From Fig.02, we see that sun goes from east to west, and during the winter sun is mostly inclined towards south, and travels through near the zenith in the middle of the year.

D. Typical meteorological year (TMY) data

The intensity of the sun on earth surface varies over time based on the sun distance, and the amount of atmospheric distance sunlight travels before reach the earth surface. The National Solar Radiation Data Base (NSRDB) archives have directly recorded TMY data for different location over the whole United States. In TMY dataset, Direct Normal Irradiance (DNI) and Diffuse Horizontal Irradiance (DHI) are available for every hours of a year. DNI is the amount of solar radiation received by a surface in per unit area, which is held perpendicular to the incoming sunlight. On the other hand, DHI is the amount of diffuse radiation received by a horizontal surface in per unit area, which is due to the scattered-sunlight, comes equally from the all direction over the whole sky. The TMY datasets are available for public download at National Renewable Energy Laboratory (NREL) website [7].

E. Direct radiation model

Direct sunlight is one form of getting solar energy by patches, which can be estimated by the direct radiation model. A patch may get the direct sunlight or may be cast by the shadow at a specific time of the day. Therefore, at first, a shadow map was generated for a given sun position over the whole scene.

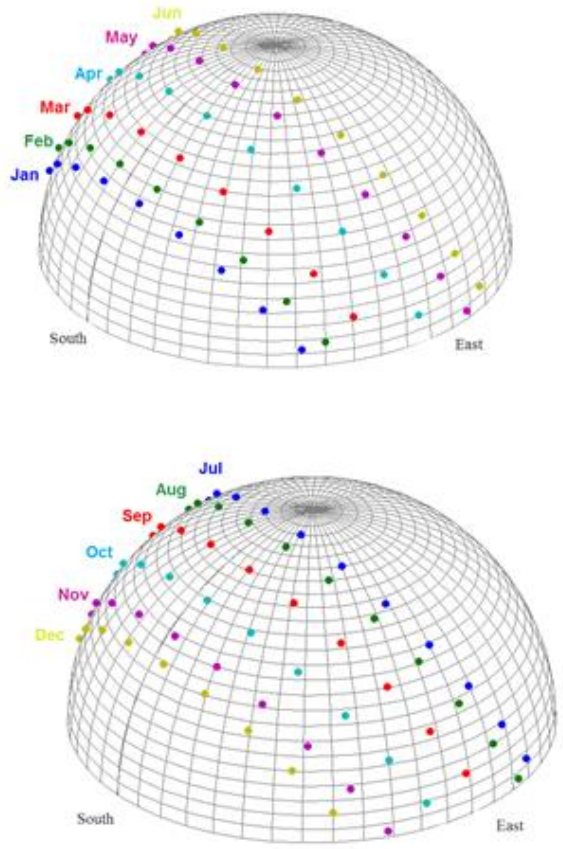

Fig. 3. Position of the sun on the sky at different day of the year in DFW area. First day of January to June (Top), first day of July to December (Bottom).

Since sunray lines are parallel to each other, and an object in one ray line can only cast a shadow in the same ray line, not in any others. In Fig.4, ray lines are shown for two different solar azimuths—0 degrees, and 330 degrees. In the left side of Fig.4, ray lines are shown for the zero degrees azimuth; different colors represent separate ray lines. It is clear that all sunrays are coming from north to south direction. In the right side of the Fig.4, sunrays are coming from 330 degrees azimuth. As this ray lines are drawn over a digitized raster, the quantization effect can be seen in the right side figure.

Each ray line had a starting point at the scene—the first patch of the scene a sun ray encounter. Using trigonometry, the minimum height required to avoid the shadow by the next patch in the same ray line was calculated. This is named the shadow limit for that patch. If all points of a patch were below the shadow limit, then it was considered as a patch under the shadow; in that case, the same shadow limit was used to calculate the shadow limit of the next patch in that ray line. On the other hand, the patch was considered as lighted if any point of the patch was above the shadow limit. In that case, the height of the current patch was used as the new shadow limit, and the shadow limit for the next patch was calculated accordingly. This shadow calculation method is fast because it handles each patch only one time. Facade patches were

segmented in multiple patches as we described in patch building section. Only patches which were below the shadow limit were considered as the shaded patches, patches above the shadow limit were considered as the lighten patches.

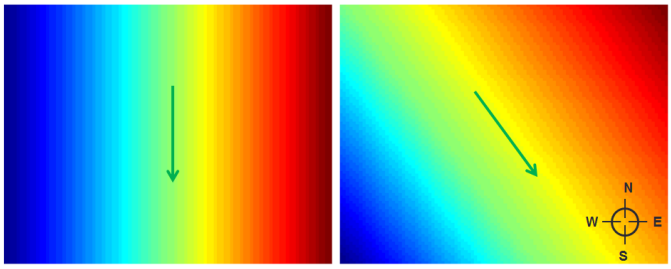

Fig. 4. Raylines are shown in different colors, same color means same raylines. Raylines map for solar azimuth zero(Left) and solar azimuth 330(right).

In Fig.5, the shadow limit and the shadow cast by patches are shown for two different solar elevation angles. From shadow limit figures on the left, we see that shadow limit is higher just after the tall buildings, and gradually decreasing based on the solar elevation angle. In the right side figures, the potential areas of shadow are shown in blue color. The shadows of the buildings were taller in top figures where elevation angle was smaller—the sun was close to the horizon. One thing to note that facades facing opposite side of the sun were also in the shaded region, but those will be calculated in the next step.

After calculating the potential shadow location, solar intensity on each patch without shadow was calculated. The received solar intensity of a patch can be determined by the angle between the sunray and the normal of the patch. The patch will get the highest direct solar intensity if the sunray is perpendicular to the patch, which is the DNI value of that hour

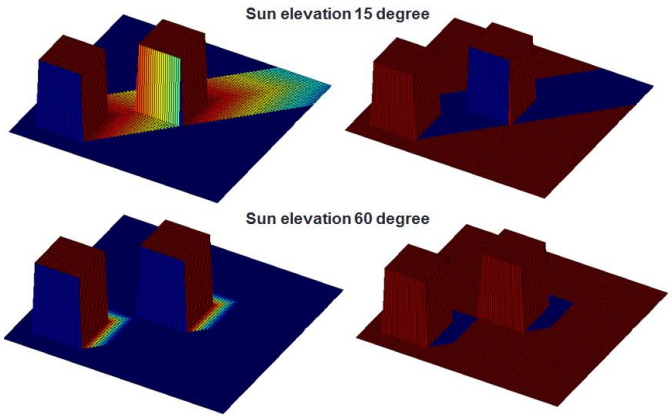

Fig. 5. Shadow limit are shown in color in elevation map (Left). Shadows due to occlusion are shown in right. Lower elevation angle leads to taller shadows.

from the TMY data. The received intensity is calculated as follows,

$$I = DNI(\cos(sunElevation) \times \sin(patchTilt) \times \cos(sunAzimuth - patchAzimuth) + \sin(sunelvation) \times \cos(patchTilt))$$

Here, $patchTilt$ is zero for flat patches, and 90 degrees for vertical patches.

In Fig.6, received intensity by patches is shown for four different angles, where DNI was set as 1. From the figure, we see that for lower elevation angles, when the sun was at the horizon, facades facing that direction received more sunlight than flat patches. On the other hand, for higher elevation angles—sun close to the zenith, flat patches received more sunlight than facades.

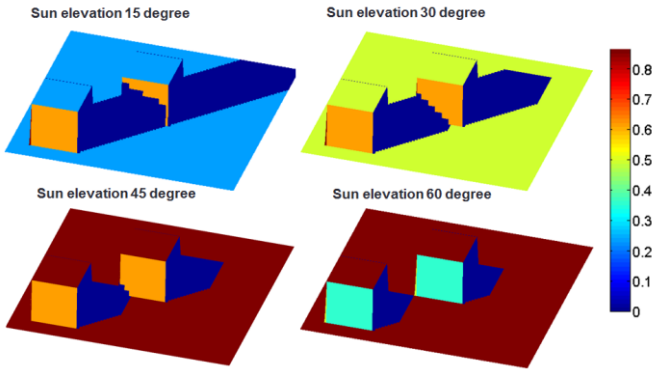

Fig. 6. Solar intensity by direct sunlight for four different solar elevation angles. For lowesr elevation angles, casted shadows are small. Shadows are casted on facades too.

F. Diffuse radiation model

Additional to direct sunlight, another form of solar power reception by any surface is the diffuse radiation. This is the amount of solar power received by the surface from all over the sky. Diffuse Horizontal Irradiance (DHI) in TMY data is the amount of diffuse radiation per unit area received by a flat surface if the whole sky can be seen from that surface. Many patches did not have the full view of the sky because of occlusion and orientation. In this diffuse model, the whole sky was segmented in 1081 region, from 15 to 90-degree elevation and 0 to 360-degree azimuth using 5 degrees increment. All the segments are shown in Fig .7 on the half hemisphere.

The previous shadow mapping algorithm was used for these 1081 separate sources to find shadows. The shadow map is a binary map representing shadow and no shadow region. Sky view factor was calculated by averaging these 1081 shadow maps, where one mean the patch get the full view of the sky and zero means the whole sky is out of sight from that patch. The sky view factor for the test data is shown in Fig.8. From Fig.8, we see that all of the facades have sky view factor not more than half. The vertical facades miss the half of the hemisphere because of its orientation, and if there is any adjacent building then the occlusion reduced the sky view factor less than the half. Additionally, sky view factor increased gradually far from the buildings and became one for flat surfaces without any occlusion.

III. RESULTS

The proposed method was applied on a 187m^2 urban area in the DFW region. A 2m-by-2m-elevation raster was created from LiDAR point cloud, where data density was 4 points/m^2. The solar potential was estimated in one-hour intervals for a whole year. In this section, we are going to make some conclusion from this estimation results.

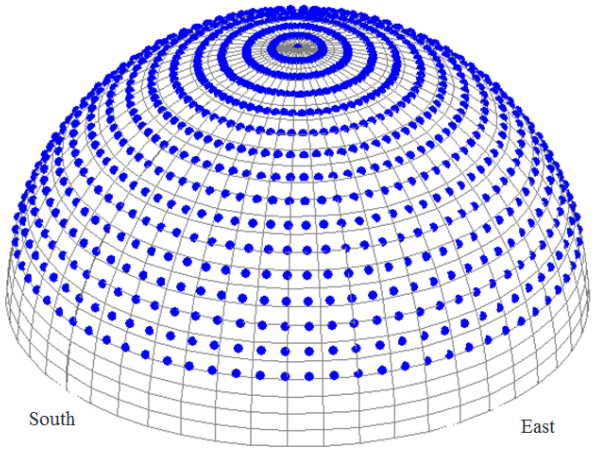

Fig. 7. To calculate sky view factor, 1081 sources were consider all over the sky. All sourcs are shown in sky half hemisphere.

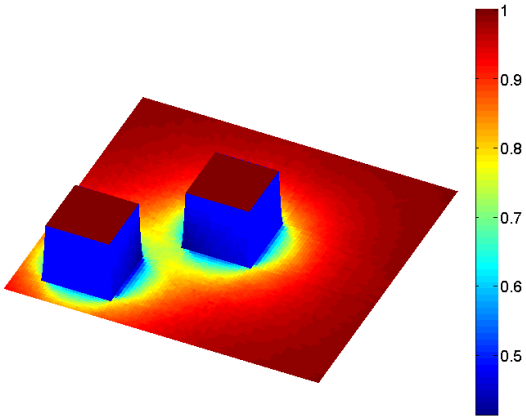

Fig. 8. Sky view factor on the test dataset. Facades have sky view factor below 0.5 because half of the sky was out of sight for vertical facades.

In Fig.9, the on average daily solar potentials are shown for four different months of the year. In the middle of the year, the summer season in Texas, the solar potential was highest in the whole area. The solar potential was gradually increased from the beginning to the middle of the year and then gradually decreased at end of the year. It can be also noted that south-facing facades received the most solar potential, and the north-facing facades received the least solar potential because the sun is tilted toward the south side. In the end and beginning of the year, south facades received the most solar potential.

In Fig.10, the annual solar potential is shown from two different angles with enlargements of the same area. It can be seen that the building facades also received a significant amount of solar potential, where south facing facades received the highest amount of sunlight. From annual solar potential estimation, we can also conclude that the south facing walls received the most sunlight over the whole year.

For better analysis, facades are grouped as north-facing, south-facing, east-facing, and west-facing facades. In Fig.11, daily solar potential over facades facing in four sides is shown. South facing facades received the highest solar potential almost all over the year, except during summer. In summer, south-facing and north-facing facades received almost the same amount of solar potential. Although, east-facing and west-facing facades received the highest amount of solar potential in the summer time because of long day hour and higher solar intensity at the period of the year. Therefore, south-facing facades are the most preferable, and then east-facing and west-facing facades are preferable for solar panel installation for this area.

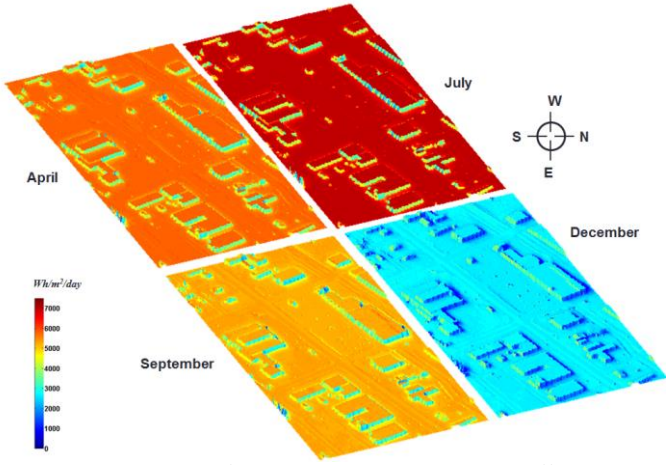

Fig. 9. Average amount of solar power received per day at different months of the year. Solar power reception was the highest during summer season.

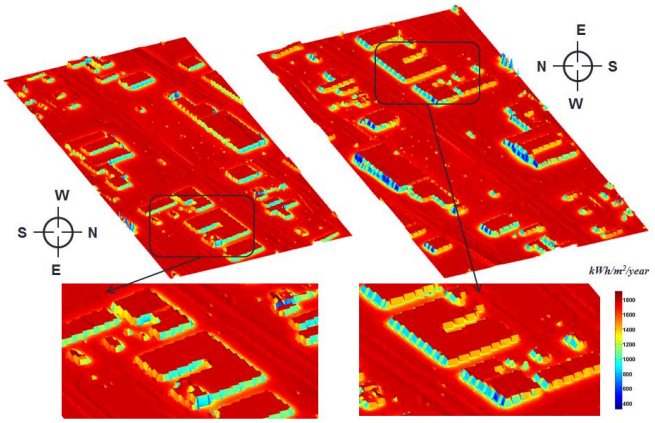

Fig. 10. Annual solar power received per square meter on the dataset. Two different angles and two zoomed versions are shown for better visualization.

Finally, the amounts of solar potential received by facades facing four different sides are compared with the rooftop solar potential in Fig.12. We see that south-facing facades received 1 to 1.4 times more solar potential than rooftops during winter season. Although, during summer solar power received by the south-facing sides drastically went below the solar power received by the east and west facing facades. East and west facing facades received almost same amount of solar power over the whole year. It can be noted that north-facing facades received the lowest amount of solar power among all facades.

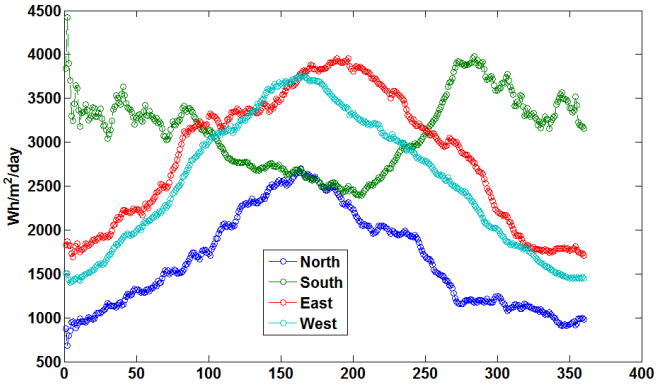

Fig. 11. Daily average solar power received by differet facades.

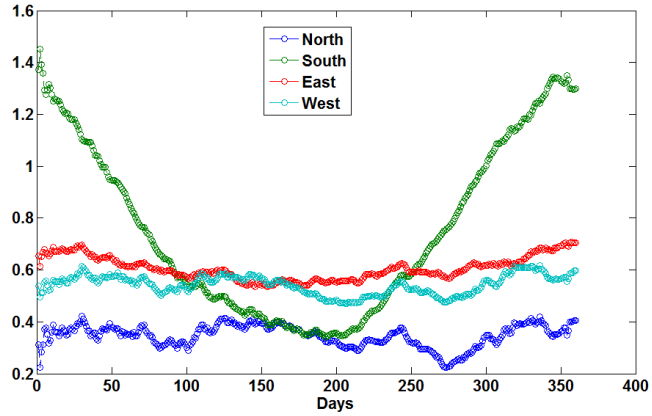

Fig. 12. Solar potential received by different facades compared to the rooftops over the year.

IV. Conclusions

First, facades can significantly contribute to accommodate space for solar panel installation. South facing facades received the highest amount of solar power among all facades. Interestingly, south facing facades received more solar energy than rooftops during winter season.

In future, the tool will be adapted for very large scale batch processing. The source code will make available in public domain at VEL at UTA website.

References

[1] Pinde Fu, and Paul Rich, "Design and implementation of the Solar Analyst: an ArcView extension for modeling solar radiation at landscape scales." In Proceedings of the 19th Annual ESRI User Conference, vol. 1, pp. 1-31. 1999.

[2] Jaroslav Hofierka, and Marcel Suri, "The solar radiation model for Open source GIS: implementation and applications." In Proceedings of the Open source GIS-GRASS users conference, vol. 2002, pp. 51-70. 2002.

[3] P. Redweik, C. Catita, and M. Brito. "Solar energy potential on roofs and facades in an urban landscape." Solar Energy 97 pp.332-341, 2013.

[4] C. Carneiro, "Extraction of urban environmental quality indicators using LiDAR-based Digital Surface Models." Thèse École polytechnique fédérale de Lausanne EPFL, PhD thesis, 2011.

[5] P. Acharjee, G. Toscano, and V. Devarajan, "A novel angular filter based LiDAR point cloud classification," ASPRS annual conference, Tampa, Florida, 2015.

[6] C. Honsberg, and S. Bowden, "Photovoltaic Education Network", Retrieved March 06, 2017 from http://www.pveducation.org/pvcdrom/2-properties-sunlight/suns-position.

[7] National Solar Radiation Data Base, Retrieved March 06, 2017 from http://rredc.nrel.gov/solar/old_data/nsrdb/1991-2005/tmy3/